Journal of Fish Biology (2008) **73,** 1946–1959
doi:10.1111/j.1095-8649.2008.01998.x, available online at http://www.blackwell-synergy.com

Embryonic stages and eye-specific gene expression of the local cyprinoid fish *Anabarilius grahami* in Fuxian Lake, China

L. Ma*†‡, X. F. Pan§‡, Y. H. Wei*†, Z. Y. Li§, C. C. Li*, J. X. Yang§‖ and B. Y. Mao*‖

**CAS-Max Planck Junior Scientist Group, State Key Laboratory of Genetic Resources and Evolution, Kunming Institute of Zoology, Chinese Academy of Sciences, Kunming 650223, China, †Department of Systematic Zoology, Graduate University of Chinese Academy Sciences, Beijing 100039, China, and §State Key Laboratory of Genetic Resources and Evolution, Kunming Institute of Zoology, Chinese Academy of Sciences, Kunming 650223, China*

(Received 12 March 2008, Accepted 12 June 2008)

Anabarilius grahami is a cyprinoid fish endemic to Fuxian Lake, Yunnan, China. In this study, a comprehensive staging series of *A. grahami* was produced. The embryonic development of *A. grahami* was divided into six main periods: zygote period, cleavage period, blastula period, gastrula period, segmentation period and hatching period. Its embryonic development is essentially similar to that of zebrafish *Danio rerio* but relatively slower. The expression patterns of *A. grahami sox2*, *pax6a*, *six3a* and *rx2* genes were also cloned and checked during eye development. The four genes showed similar expression patterns to their *D. rerio* homologues, suggesting the evolutionary conservation of the regulatory network of eye development.

Key words: *Anabarilius grahami*; developmental stages; expression pattern; eye-specific gene; *pax6a*; *six3a*.

INTRODUCTION

Fishes have been important models for the study of vertebrate embryogenesis. Especially, the zebrafish *Danio rerio* (Hamilton) and the medaka *Oryzias latipes* (Temminck & Schlegel, 1846) have become widely used model organisms, and their embryological development is considered representative for teleosts (Westerfield, 2000). The developmental stages in these species have been described in great detail. The developmental stages have also been reported in some other representative fish species, *e.g.* the loach *Misgurnus anguillicaudatus* (Cantor) (Fujimoto *et al.*, 2006), the summer flounder *Paralichthys dentatus* (L.) (Martinez & Bolker, 2003), the Atlantic cod *Gadus morhua* L. (Hall *et al.*, 2004), *etc.* These data have contributed to the general understanding of fish development

‖Authors to whom correspondence should be addressed. Tel.: 86-871-5198989; fax: 86-871-5193137; email: mao@mail.kiz.ac.cn

and the developmental basis of differences between closely related species. In fact, fishes have become valuable models in evolutionary developmental biology to reveal the molecular basis of evolutionary novelty and adaptation. Also, these data are valuable for the protection of endangered species and the production of economically important species.

Anabarilius (Cockerell, 1923) is a genus of ray-finned fish of the Cyprinidae and is found only in south-west China. Because of difficulties in obtaining complete developmental series of the *Anabarilius* species, their early development remains poorly understood. *Anabarilius grahami* (Regan) (Fig. 1) is endemic to Fuxian Lake, Yunnan, China. So far, only a few reports on its ecology and phylogeny are available. Fuxian Lake is the second deepest lake of China and was formed in the late Pliocene (3·0–3·4 million years ago) as a result of fault depressions (Ley *et al.*, 1963; Yang, 1984). Since its formation, the lake has generally followed a deepening and oligotrophic development that has produced profound effects on the biological characters of *A. grahami*. For example, *A. grahami* prefers to breed at outlets of cave springs or hill springs where the substrate and water current are similar to hill streams. *Anabarilius grahami* has a long annual breeding season (March to October) and temporally regular interval (*c.* 7 days) between two sequent spawning populations. The larvae and adults of *A. grahami* occupy different living spaces, with the larvae, and juvenile occur in shallow coastal regions and adults in the middle and upper layers of open water. These habits can ensure enough food for the larvae and full use of the limited breeding sites and have been suggested to be an adaptation to the oligotrophic environment of the lake. The population of *A. grahami* is female dominant with a sexual ration of 4·1:1 (female:male). Dominant females can ensure a potentially high fecundity for the population (Yang, 1992). The adult *A. grahami* is 120–246 mm in length. It used to be the main fish product in Fuxian Lake and is economically important. However, because of the invasion of alien fish species and excessive capture, the production of *A. grahami* has declined greatly in recent years. To protect and study this valuable species, the authors have succeeded in the artificial cultivation of *A. grahami.*

In this article, first a comprehensive staging series of early development was presented in *A. grahami*. The embryonic development of *A. grahami* was divided

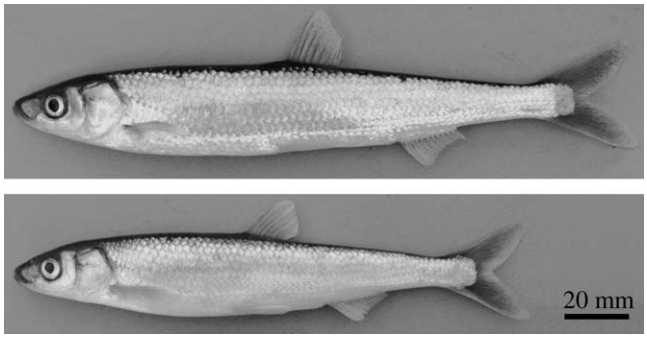

FIG. 1. A female (upper panel) and a male (lower panel) adult *Anabarilius grahami*. The female (197 mm in total length) is bigger than the male (161 mm in total length). Scale bar = 20 mm.

into six main periods: zygote period, cleavage period, blastula period, gastrula period, segmentation period and hatching period. Stages from fertilization to hatching were named descriptively following the *D. rerio* staging system (Kimmel *et al.*, 1995) based on the landmark morphological features.

Vertebrate eye development is controlled by a complex regulatory network. The neural plate is firstly induced by the underlying mesoderm during the gastrula stage as indicated by the expression of the early neural marker Sox2. The eye development is initiated at the early neurula stage with the determination of the retina anlage in the anterior neural plate. Subsequently, the initially single eye field splits into two symmetric retinal primordia that evaginate laterally from the forebrain and form the optic vesicles (Jean *et al.*, 1998). Several transcription factors that pattern the anterior neural plate of the early vertebrate embryo such as Pax6, Rx and Six3 are essential for normal eye development. Sox2 also plays important roles in eye development. To gain insight into the eye development of *A. grahami*, the expression patterns of *sox2*, *pax6a*, *six3a* and *rx2* genes were checked during its embryonic development.

MATERIALS AND METHODS

ANIMALS

Newly fertilized eggs of *A. grahami* fish were collected from the Fuxian lake of Yunnan Province, China. Two clutches of newly fertilized eggs from different females were collected during July 2007.

ANABARILIUS GRAHAMI DEVELOPMENTAL STAGING

The fertilized eggs were cultured at 20° C, and the embryos were staged according to their morphological characteristics following that of *D. rerio* (Kimmel *et al.*, 1995). All images were taken under a Leica (Nussloch, Germany) dissecting stereomicroscope. All the embryos up to 48 h post-fertilization were dechorionated manually with watchmaker's forceps before taking the pictures.

ISOLATION OF *ANABARILIUS GRAHAMI SOX2, PAX6A, SIX3A AND RX2* FRAGMENTS

Anabarilius grahami sox2, *pax6a*, *six3a* and *rx2* fragments were cloned by reverse transcription polymerase chain reaction (RT-PCR). Total RNAs from mixed stages of *A. grahami* embryos were prepared using the Trizol reagent (Invitrogen, Carlsbad, CA, U.S.A.). The first strand cDNA was prepared using the RevertAid™ H minus first strand cDNA Synthesis kit (MBI Fermentas, Vilnius, Lithuania) and oligo (dT) primers. Primers for *A. grahami sox2*, *pax6a*, *six3a* and *rx2* were designed according to conserved regions of the *D. rerio* homologous genes. The primers used for polymerase chain reaction (PCR) were as follows (product sizes in parentheses): *sox2*: forward 5′-AAGCTTCTT-CATGGTGTGGTCGAGGG-3′ and reverse 5′-CATACTGATCATGTCCCGCAGG-3′ (691 bp); *pax6a*: forward 5′-ACCTGGCTAGCGAAAAGCAACAG-3′ and reverse 5′-CAGTATTGGGACATGTCTGGTTC-3′ (856 bp); *six3a*: forward 5′-GTCTGCGA-GACGCTGGAGGA-3′ and reverse 5′-ATACGTCGCATTCCGAGTCACT-3′ (716 bp); *rx2*: forward 5′-CACAGCATCGACGTCATTCTGGG-3′ and reverse 5′-CTGAATGTGCTCCTTGGCCTTCA-3′ (852 bp). The PCR products were cloned in the pGEM-T Easy vector (Promega, Madison, WI, U.S.A.) and sequenced. The sequences

were submitted to the GenBank under accession numbers EU725603 (*sox2*), EU725604 (*six3a*), EU725605 (*pax6a*) and EU725606 (*rx2*).

PROBES AND WHOLE-MOUNT *IN SITU* HYBRIDIZATION

The *in situ* hybridization was performed according to Schulte-Merker (2002) with some modifications. Sense and anti-sense digoxigenin (DIG)-labelled RNA probes for *A. grahami sox2*, *pax6a*, *six3a* and *rx2* were prepared using the pGEM-T Easy vector. Sense probes were used as controls. Embryos were fixed with 4% paraformaldehyde (PFA) in phosphate-buffered saline (PBS) overnight at 4° C. The embryos were then dechorionated with watchmaker forceps, dehydrated in methanol and stored at −20° C. Rehydrated embryos were treated with proteinase K [10 μg ml^{-1} in phosphate-buffered saline + Tween3 (PBST)] for 3–5 min at room temperature, washed twice with PBST (PBS plus 0·1% Tween) and re-fixed for 20 min with 4% PFA in PBST. The embryos were then prehybridized at 60° C for 4 h in HYB^+ (50% formamide, 5× saline sodium citrate 4 (SSC), 0·1% Tween-20, 1 mg ml^{-1} yeast RNA, 50 μg ml^{-1} heparin). Hybridization was carried out at 62·5° C for overnight in HYB^+ with different probes (1 ng μl^{-1}). The embryos were then washed twice at 60° C with 50% formamide/2× SSCT (saline sodium citrate plus 0·1% Tween, 30 min each time), once at 60° C with 2× SSC (15 min), twice at 60° C with 0·2× SSCT (20 min each) and twice with MABT (150 mM Maleic acid, 100 mM NaCl, pH 7·5, 0·1% Tween-20) at room temperature (5 min each). The embryos were incubated with blocking solution (MABT, 2% blocking reagent) for overnight at 4° C with rocking and then with anti-digoxigenin Fab-alkaline phosphatase (1:5000; Roche) in blocking solution for overnight at 4° C with gentle rocking. The embryos were washed once with MABT plus 10% sheep serum at room temperature for 25 min and eight more times (45–60 min each) with MABT at room temperature with gently shaking. Then, the embryos were washed with PBST and incubated in the Purple AP solution (Roche, Basel, Switzerland) at room temperature in the dark. When the signal had developed to the desired extent, the embryos were washed with PBST and re-fixed with 4% PFA in PBS. The stained embryos were kept in PBS and observed with a Leica MZ 16 stereomicroscope.

RESULTS

ANABARILIUS GRAHAMI DEVELOPMENTAL STAGING SERIES

Embryonic development of *A. grahami* at 20° C was divided into six main periods: zygote period, cleavage period, blastula period, gastrula period, segmentation period and hatching period. Staging of the embryos was performed following the general teleost staging scheme suggested by (Kimmel *et al.*, 1995). The developmental stages are described below, and the corresponding timing is summarized in Table I.

Zygote period (0–40 min)

The zygote period began with the fertilization of the oocyte and ended with the first cleavage at *c.* 40 min. The diameter of the zygote was *c.* 1·4 mm. When the oocyte was laid, the chorion still closely surrounded the cell and the cytoplasm was not separated from the yolk within 10 min after fertilization. The yolk-free cytoplasm gradually segregated to the animal pole and the blastodisc formed at *c.* 30 min post-fertilization [Fig. 2(a), (b)].

Cleavage period (40 min–2 h 50 min)

The first cleavage occurred at *c.* 40 min after fertilization. After the first cleavage, the blastomeres divided synchronously at intervals of *c.* 15–35 min

TABLE I. Developmental stages of *Anabarilius grahami* at 20° C

Stage name	Time	Characteristics	Figure number
Zygote period			Fig. 2(a), (b)
1-cell	0000 hours	Yolk-free cytoplasm begin to segregate	
Cleavage period			
2-cell	40 min		Fig. 2(c)
4-cell	1 h 15 min		Fig. 2(d)
8-cell	1 h 50 min		Fig. 2(e)
16-cell	2 h 5 min		Fig. 2(f)
32-cell	2 h 20 min		Fig. 2(g)
64-cell	2 h 35 min		Fig. 2(h)
Blastula period			
128-cell	2 h 50 min		Fig. 2(i)
256-cell	3 h 20 min		Fig. 2(j)
512-cell	3 h 50 min	Loss synchronicity of cell divisions; onset mid-blastula transition	Fig. 2(k)
1k-cell	4 h 20 min	Yolk syncytial layer formation	Fig. 2(l)
High	5 h 20 min	The cell mound bulging out	Fig. 2(m)
Oblong	5 h 45 min		Fig. 2(n)
Sphere	6 h	Spherical shape; flat border between blastodisc and yolk	Fig. 2(o)
Dome	7 h 35 min	Beginning of epiboly	Fig. 2(p)
30% epiboly	7 h 50 min	30% coverage of the yolk cell by the blastoderm	Fig. 2(q)
Gastrula period			
50% epiboly	8 h 30 min	Half coverage of the yolk cell by the blastoderm	Fig. 2(r)
Germ-ring	9 h	Arrest at 50% epiboly, germ ring appears	Fig. 2(s)
Shield	9 h 30 min	Embryonic shield formation, 50% epiboly	Fig. 2(t)
75% epiboly	11 h 20 min		
80% epiboly	13 h 15 min	Dorsal side distinctly thicker	
90% epiboly	13 h 30 min		Fig. 2(w)
Bud	15 h	100% epiboly, tail-bud formation and thickening at the dorsal side with the anterior presumptive brain region	Fig. 2(x)
Segmentation period			
2-somite	15 h 30 min	Brain primordium thickened into the neural keel	Fig. 3(a)
5-somite	18 h		Fig. 3(b)
6-somite	19 h	Optic primordium begins to show	Fig. 3(c)
8-somite	2000 hours	Brain primordium distinctively thickened	Fig. 3(d)

TABLE I. Continued

Stage name	Time	Characteristics	Figure number
16-somite	23 h 15 min	Somites transformation into a chevron shape	
18-somite	24 h 15 min	Otic vesicle	Fig. 3(e)
22-somite	26 h 50 min	Yolk extension, lens placode and tail extension	Fig. 3(f)
27-somite	31 h		Fig. 3(g)
31-somite	33 h	Straightening of posterior trunk, olfactory placode thicken	Fig. 3(h)
34-somites	36 h	The brain sculptured; the length of the yolk extension equals the yolk ball	Fig. 3(i)
44-somites	44 h	The length of yolk extension markedly surpasses the diameter of the yolk ball	Fig. 3(j)
Hatching period			
Retina–pigment	52 h	Early retina pigmentation, early touch reflex	Fig. 4(a)
High-pec	60 h	Retina pigmentation, pectoral fin rudiments	Fig. 4(b)
Long-pec	72 h	Elongated pectoral fin buds	Fig. 4(c)
Pec-fin	84 h	Mouth open, pectoral fin, pharyngeal arches	Fig. 4(d)
Protruding-mouth	96 h	Mouth protruding	
Early larva	4–7 days	The pigmentation increases; eating food	Fig. 4(e)

(Table I). The cleavage period includes the 2-, 4-, 8-, 16-, 32- and 64-cell stages [Fig. 2(c)–(h)]. The early cleavages occurred at regular orientations perpendicular to each other. At 64-cell stage, the blastodisc became bi-layered [Fig. 2(h)].

Blastula period (2 h 50 min–7 h 50 min)

The blastula period began with the 128-cell stage and ended with the beginning of the gastrulation. The blastula period includes 128-cell stage, 256-cell stage, 512-cell stage, 1000-cell stage, high stage, oblong stage, sphere stage, dome and 30% epiboly stage [Fig. 2(i)–(q)]. The cell divided more or less synchronously during the early stages of the blastula period. From the 512-cell stage on, the cell mound became more compact and lost the synchronicity of cell division, the mid-blastula transition occurred. The yolk syncytial layer formed at the 1000-cell stage at the margin of the blastodisc. At the sphere stage, the border between the blastodisc and the yolk was considerably flattened. At the dome stage, the blastoderm formed a dome-like shape because of the bulging up of the yolk cell towards the animal pole and the epiboly began. At 30% epiboly, the blastoderm covered *c.* 30% of the yolk cell. In the *A. grahami* embryo, the blastula was a solid mount of cells without a blastocoele as in *D. rerio* (Kimmel *et al.*, 1995).

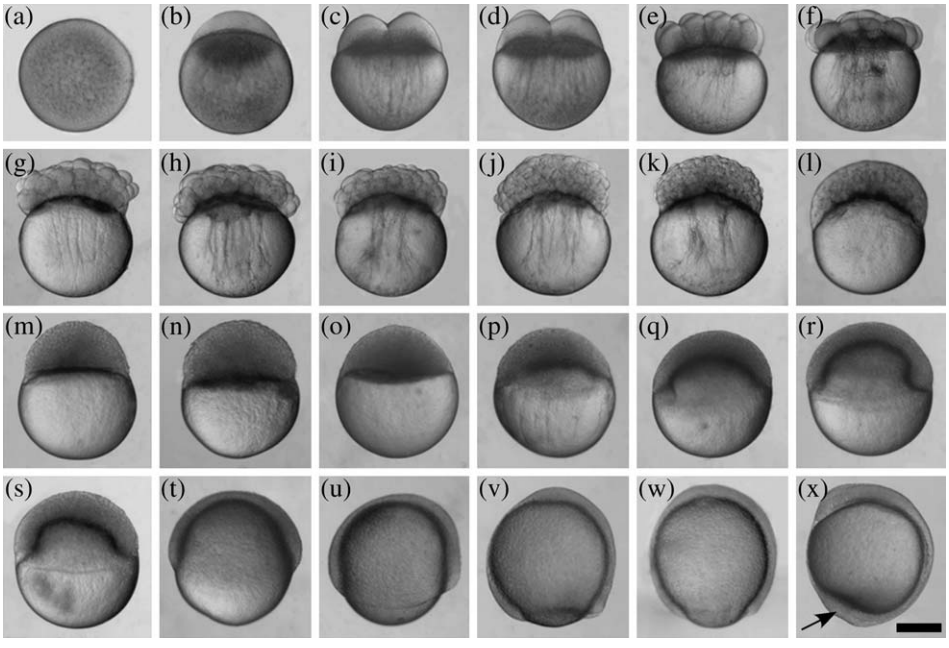

FIG. 2. Embryonic development of *Anabarilius grahami* during the zygote, cleavage, blastula and gastrula periods. (a) The zygote, a few minutes after fertilization, (b) The zygote *c.* 30 min after fertilization, yolk-free cytoplasm has begun to segregate to the animal pole, (c) 2-cell stage, (d) 4-cell stage, (e) 8-cell stage, (f) 16-cell stage, (g) 32-cell stage, (h) 64-cell stage, (i) 128-cell stage, (j) 256-cell stage, (k) 512-cell stage, (l) 1000-cell stage, (m) high stage, (n) oblong stage, (o) sphere stage, (p) dome stage, (q) 30% epiboly stage, (r) 50% epiboly stage, (s) germ ring stage, (t) shield stage, (u) 70% epiboly stage, (v) 85% epiboly stage, (w) 90% epiboly stage and (x) bud stage, arrow shows the tail bud. Scale bar = 0·5 mm.

Gastrula period (8 h 30 min–15 h 30 min)

In the gastrula period, extensive cell movements were observed, including involution, convergence and extension, generating the three primary germ layers and the embryonic axes. Gastrulation began with cell involution at around 50% epiboly [Fig. 2(r)]. The blastoderm thickened at the leading edge all around the blastoderm rim giving rise to the germ ring [Fig. 2(s)]. On the future dorsal side of the embryo, the embryonic shield formed as a local accumulation of cells at one position of the germ ring [Fig. 2(t)]. Epiboly stopped at 50% until late shield stage. As soon as the shield had formed, epiboly proceeded at a relatively constant rate until the blastoderm completely covered the yolk, reaching the 100% epiboly [Fig. 2(x)]. As epiboly continued, the shield became progressively less distinctive. The gastrula period ended when epiboly is complete. The tail bud then appeared as a distinct thickening at the caudal end of the embryo, near the site yolk plug closure [Fig. 2(x)].

Segmentation period (15 h 30 min–52 h)

The segmentation period was characterized by the sequential formation of the somites, and this period lasted to just prior to hatching. During this period,

the embryo elongated along the anterior–posterior axis, the tail bud developed longer and rudiments of the primary organs became apparent. Somites formed in bilateral pairs, as the developing embryo extends posteriorly. The first somite was observed in the central part of the embryo at *c.* 15·5 h post-fertilization (hpf). At 2-somite stage, the length of the embryo was *c.* 1·3 mm, the same as the zygote [Fig. 3(a)]. The optic primordium can firstly be distinguished at the 6-somite stage from a side view [Fig. 3(c)] and became very clear with a prominent horizontal crease at 8-somite stage [Fig. 3(d)]. Brain morphogenesis started during the first half of the segmentation period. At 18-somite stage, the otic placode appeared beside the hindbrain rudiment; the tail rudiment extended and most of the somites showed the characteristic myotomal V-shape [Fig. 3(e)]. At 22-somite stage, the yolk extension became distinguished from the anterior yolk ball; the length of the yolk extension was about half the diameter of the yolk ball. The lens placodes appeared in the centre of the optic vesicles, and the otic vesicles were also distinguishable [Fig. 3(f)]. The tail bud began to lift from the body of the embryo [Fig. 3(f)]. At 27-somite stage [Fig. 3(g)], the length of the yolk extension became similar to that of the yolk ball. The somitogenesis was complete at *c.* 44 hpf, and the total somite number in *A. grahami* was *c.* 44. At this stage, the anterior brain of embryo had displayed all major subdivisions [Fig. 3(j)].

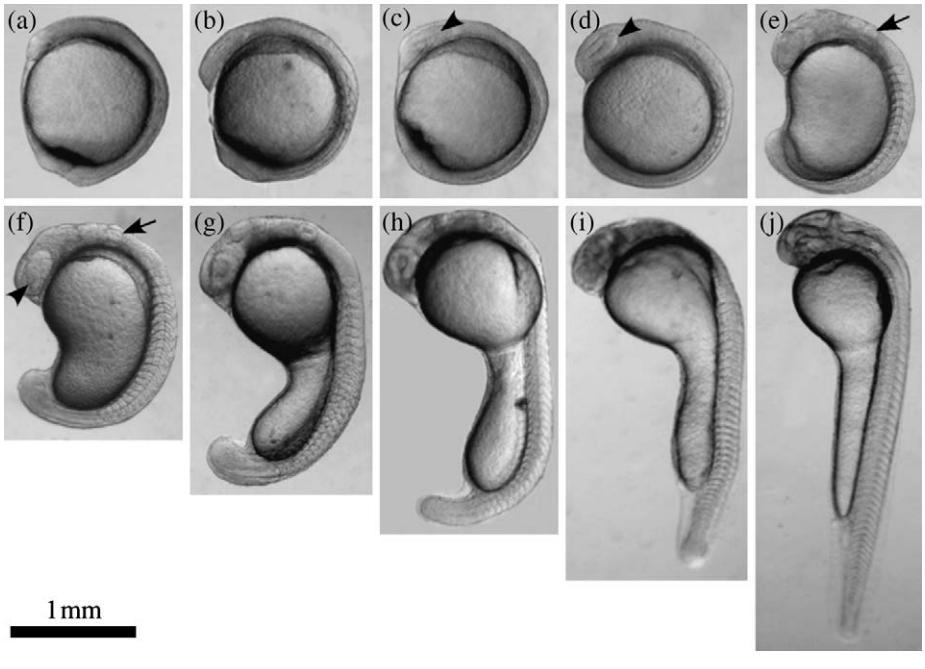

FIG. 3. Embryonic development of *Anabarilius grahami* during the segmentation period. (a) 2-somite stage, (b) 5-somite stage, (c) 6-somite stage, arrowhead indicates the optic primordium, (d) 8-somite stage, arrowhead indicates the optic vesicle, (e) 18-somite stage, arrow indicates the otic vesicle, (f) 22-somite stage, arrow indicates the otic vesicle and the arrowhead indicates the lens vesicle, (g) 27-somite stage, (h) 31-somite stage, (i) 34-somite stage and (j) 44-somite stage. Scale bar = 1 mm.

Hatching period (52–96 h)

Hatching in *A. grahami* was not synchronous, in that the embryos from a single spawning could hatch at irregular intervals as have been documented in many fishes (Balon, 1990; Penaz, 2001). The hatching period was divided into five stages: retina–pigment stage [Fig. 4(a)], high-pec stage [Fig. 4(b)], long-pec stage [Fig. 4(c)], pec-fin stage [Fig. 4(d)] and protruding-mouth stage. The majority of the organ rudiments were formed by this stage, and the development of the jaw, the gill arches and the pectoral fins were characteristic features of this period. At the retina–pigment stage, visible pigment granules appeared at the pigmented layer of the retina [Fig. 4(a)]. The rudiments of the pectoral fins appeared at the high-pec stage, and the length of the yolk extension was *c.* 1.5 times the diameter of the yolk ball [Fig. 4(b)]. At long-pec stage, the rudiments of the pectoral fins elongated caudal to the ear and the mouth was located mid-ventrally between the eyes [Fig. 4(c)]. At the pec-fin stage, the pectoral fin became a flat blade and the yolk ball became markedly smaller [Fig. 4 (d)]. The mouth migrated anteriorly during the entire hatching period, and by 96 hpf, the anterior tip of the mouth had protruded beyond the eyes [Fig. 4(e)]. Moreover, the embryos became sensitive to touch at this period. In the present

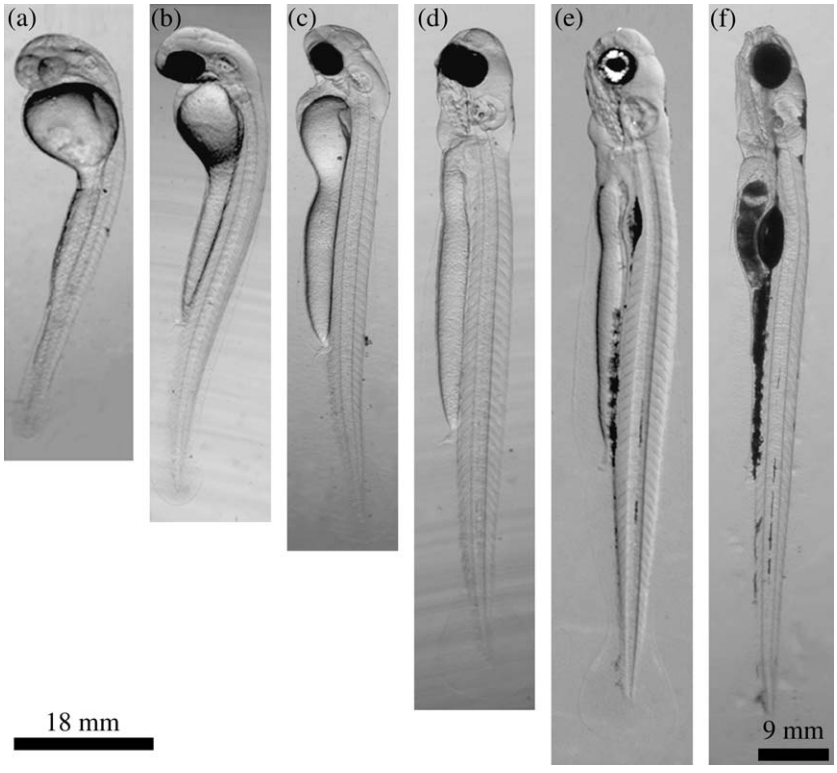

FIG. 4. Development of *Anabarilius grahami* during the hatching, larval and early juvenile period. (a) Retina–pigment stage, (b) high-pec stage, (c) long-pec stage, (d) pec-fin stage, (e) early larval period (96 h) and (f) early juvenile (20 days). Scale bar in (f) = 1 mm.

study, hatching occurred over a period of 44 h with the earliest embryos to hatch, displaying poor swimming capabilities.

Early larval period (4–7 day)

At the early larval period, most of the morphogenesis in the developing *A. grahami* was complete. The mouth continued to grow out more dorsally and anteriorly. The pigmentation appeared both in surface areas of the head and near the lateral line at the posterior part of the body. The larvae started to swim actively. In addition, they now showed escape responses, respiration movements, and they started looking for and eating food [Fig. 4 (e)]. At the early juvenile period, the jaws protruded more anteriorly in front of the eyes [Fig. 4(f)].

CLONING AND DEVELOPMENTAL EXPRESSION OF *A. GRAHAMI SOX2, PAX6A, SIX3A* AND *RX2* GENES

Partial sequences of *A. grahami sox2*, *pax6a*, *six3a* and *rx2* were cloned through RT-PCR, showing 94, 93, 96 and 83% identities with their *D. rerio* homologous, respectively. A phylogenetic analysis using the sox2 protein sequences from available fish species showed a close relationship between *D. rerio* and *A. grahami*. Whole-mount *in situ* hybridizations were carried out to investigate the embryonic expression patterns of the four eye marker genes.

At the tail-bud stage, *sox2* was strongly expressed in the presumptive forebrain and hindbrain regions but was very weak in the presumptive mid-brain and spinal cord regions [Fig. 5A(a)]. At 5-somite stage, its expression could be detected in the whole brain region and remained weak in the spinal cord [Fig. 5A(b), (b′)]. At 8-somite stage, its expression became clear also in the posterior spinal cord. From 8-somite stage on, it was strongly expressed in the developing optic vesicles. From 27-somite to 44-somite stages, it was detected in different regions in the brain, anterior spinal cord, retina, lens and the otic vesicles. Its expression became very weak in the middle and the posterior spinal cord [Fig. 5A(b)–(f)].

Pax6a expression was first detected in two bilateral triangular-shaped regions in the anterior neural plate at tail-bud stage [Fig. 5B(a), (a′)], which represented the presumptive diencephalon region, but not in the most anterior region of the neural plate. At 5-somite stage, it was expressed in the presumptive diencephalon and hindbrain but not in the mid-brain region [Fig. 5B(b), (b′)]. From 8 to 18-somite stages, *pax6a* was detected strongly in the evaginating optic vesicles, diencephalon and anterior spinal cord [Fig. 5B(c), (c′), (d), (d′)]. From 27-somite to 44-somite stage, the *pax6a* expression was found prominent in the forebrain, hindbrain, retina, lens and the anterior part of the spinal cord [Fig. 5B(e), (e′), (f), (f′)].

At tail-bud stage, *six3a* was weakly expressed in a U-shaped domain surrounding the anterior end of the neural plate [Fig. 5C(a), (a′)]. Its expression in the forebrain region became stronger at 5-somite stage [Fig. 5C(b), (b′)] and was confined to the optic vesicles and telencephalon region at 8- to 18-somite stages [Fig. 5C(c), (c′), (d), (d′)]. At 27- to 44-somite stages, the

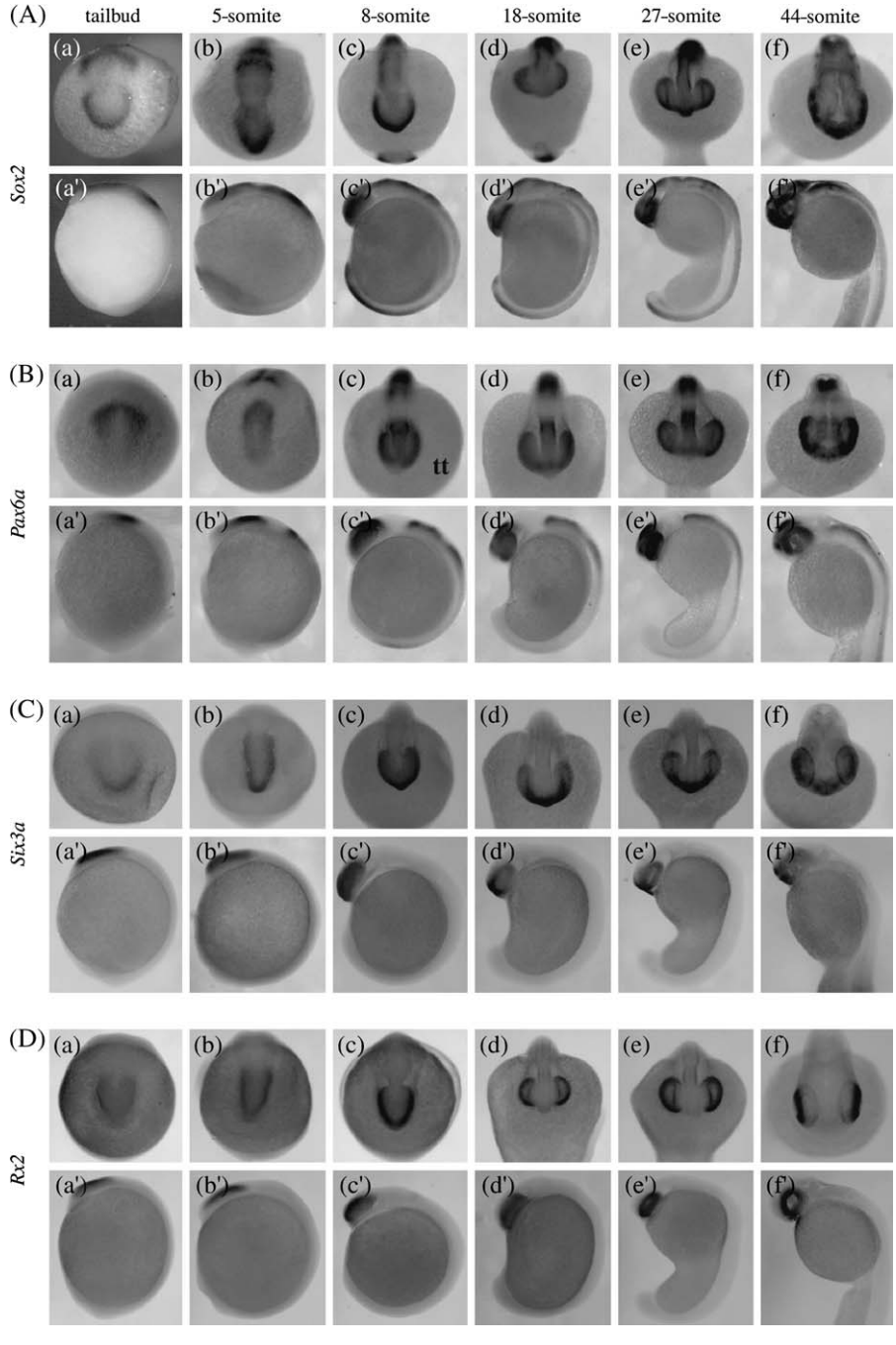

FIG. 5. The expression patterns of *Anabarilius grahami Sox2*, *Pax6a*, *Six3a* and *Rx2* from the bud stage to the 44-somite stage of embryonic development. (A) *Sox2*, (B) *Pax6a*, (C) *Six3a*, (D) *Rx2*, (a) tail-bud stage, (b) 5-somite stage, (c) 8-somite stage, (d) 16-somite stage, (e) 27-somite stage and (f) 44-somite stage. (a)–(f) frontal view, (a′)–(f′) lateral view.

expression of *six3a* was maintained in the retina, lens and restricted areas in the telencephalon [Fig. 5C(e), (e′), (f), (f′)].

Anabarilius grahami rx2 was expressed in the anterior neural plate at tail-bud and 5-somite stages [Fig. 5D(a), (a′), (b), (b′)] similar to *six3a*. At later stages, its expression was gradually confined to the developing optic vesicles and no longer in the telencephalon region [Fig. 5D(c), (c′), (d), (d′)]. At 27- to 44-somite stages, it was detected throughout the neural retina and not in the lens [Fig. 5D(e), (e′), (f), (f′)].

DISCUSSION

In this article, for the first time a comprehensive staging series was present during early development of *A. grahami*. Table I summarizes the embryonic stages of development in the *A. grahami*. Stages from fertilization to hatching were designated following the general teleost staging scheme suggested by Kimmel *et al.* (1995). The embryonic development in *A. grahami* is essentially similar to the process described in *D. rerio*, but is relatively slower than *D. rerio*, probably because of its bigger size and lower developmental water temperature. The number of somite is usually used to define developmental stages because of its periodic increase during embryogenesis. However, the final number of somite is usually species specific (Gorodilov, 2004). Thus, the organogenesis process might occur at different somite stages in different fish species (Fujimoto *et al.*, 2006). *Anabarilius grahami* (44 somites) has more somites than *D. rerio* (30–34 somites; Kimmel *et al.*, 1995). The optic primordium, otic placod and lens placode appear in *A. grahami* at 6-, 18- and 22-somite stages, respectively [Fig. 3(c), (e), (f)] while at 4-, 10- and 21-somite stages in *D. rerio* (Kimmel *et al.*, 1995). Because the authors have succeeded in the artificial culture of this species, the staging scheme for *A. grahami* embryonic and larval development should facilitate both experimental and comparative research on *A. grahami* and other Cyprinidae species and serve as a basis for more focused developmental studies. The embryos and larvae are much less pigmented in *A. grahami* than in *D. rerio*, making it a good model to study internal organogenesis.

Eye development is a complex process controlled by a network of regulatory interactions. To gain insight into the eye development in *A. grahami*, the expression patterns of *sox2*, *pax6a*, *six3a* and *rx2* genes were checked that play critical roles in eye development during early stages. Their expression patterns during embryonic development are similar to their *D. rerio* homologous (Nornes *et al.*, 1998; Seo *et al.*, 1998; Chuang *et al.*, 1999; Chuang & Raymond, 2001). The four genes are all expressed in the anterior neural plate at tail-bud stage and later prominently in the retinal progenitor cells. At later stages, all except *rx2* are also expressed in the lens. These data suggest that the molecular network involved in eye development is highly conserved in *A. grahami*.

In *D. rerio*, the *six3* and the *rx* genes are expressed initially in a uniform domain in the anterior neural plate, including the presumptive forebrain and retina regions (Seo *et al.*, 1998; Chuang *et al.*, 1999, McCollum *et al.*, 2007). Later on, they are down-regulated in the medial diencephalons region, generating two separate optic primordia. In *A. grahami*, however, the expression of *six3a* and *rx2* is very weak from the beginning in the medial region of the

anteriormost neural plate (Fig. 5). The optic primordium of *A. grahami* locates at the very anterior part of the brain region at 5- to 8-somite stages and is relatively elongated compared with *D. rerio* [Fig. 3(b–d)]. At 5- to 8-somite stages, the expression domains of *six3a* and *rx2* in the optic primordium both showed a 'U' shape [Fig. 5(b)], remain connected in the anterior tip [Fig. 5 C(b), (c), D(b), (c)]. At 18-somite stage, the two optic vesicles are separated completely as can be seen from the *rx2* expression pattern [Fig. 5D(d)]. These differences might suggest slightly different mechanisms concerning the generating of the two eye fields.

Anabarilius grahami and many other fish species in Fuxian Lake are female dominant (Yang, 1992), making it an interesting model to study the mechanisms of sex determination and their evolution. The plasticity of sex determination mechanisms is highlighted in recent fish works. Many fishes have environmentally determined sex, which can depend on factors such as temperature or social interaction (Streelman *et al.*, 2007). However, the molecular mechanisms of sex determination in fishes remain largely unknown although multiple loci (Matsuda *et al.*, 2002; Nanda *et al.*, 2002) and environmental influences are likely to be involved (Kondo *et al.*, 2006). *Anabarilius grahami* might be an appropriate model to study this question. *Anabarilius grahami* shares a most recent common ancestor with *Anabarilius andersoni* (Regan) and *Anabarilius qiluensis* (Chen & Chu) in nearby isolated Xingyun and Qilu Lakes, respectively (Yang & Chu, 1987). They might also serve as a good model to study species specification during evolution.

This study was supported by grants from the Innovation Project of Chinese Academy of Sciences (KSCX2-YW-R-090) to B.Y.M. and the National Basic Research Programme of China (2007CB411600), the National Natural Science Foundation of China (30730017) and the World Bank Dianchi Project (TF051795) to J.X.Y.

References

Balon, E. K. (1990). Epigenesis of an epigeneticist: the development of some alternative concepts on the early ontogeny and evolution of fishes. *Guelph Ichthyology Reviews* **1,** 1–48.

Chen, Y. & Chu, X. (1980). A taxonomic study on fishes of the genus *Anabarilius* from Yunnan, China. *Zoological Research* **1,** 417–424.

Chuang, J. C. & Raymond, P. A. (2001). Zebrafish genes *rx1* and *rx2* help define the region of forebrain that gives rise to retina. *Developmental Biology* **231,** 13–30.

Chuang, J. C., Mathers, P. H. & Raymond, P. A. (1999). Expression of three Rx homeobox genes in embryonic and adult zebrafish. *Mechanisms of Development* **84,** 195–198.

Cockerell, T. D. A. (1923). The scales of the cyprinid genus *Barilius*. *Bulletin of the American Museum of Natural History* **48,** 531–532.

Gorodilov, Y. N. (2004). Studies of temporal and spatial peculiarities of somitogenesis in fish embryos. *Russian Journal of Developmental Biology* **35,** 92–105.

Fujimoto, T., Kataoka, T., Sakao, S., Saito, T., Yamaha, E. & Arai, K. (2006). Developmental stages and germ cell lineage of the loach (*Misgurnus anguillicaudatus*). *Zoological Science* **23,** 977–989.

Hall, T. E., Smith, P. & Johnston, I. A. (2004). Stages of embryonic development in the Atlantic cod *Gadus morhua*. *Journal of Morphology* **259,** 255–270.

Jean, D., Ewan, K. & Gruss, P. (1998). Molecular regulators involved in vertebrate eye development. *Mechanisms of Development* **76,** 3–18.
Kimmel, C. B., Ballard, W. W., Kimmel, S. R., Ullmann, B. & Schilling, T. F. (1995). Stages of embryonic development of the zebrafish. *Developmental Dynamics* **203,** 253–310.
Kondo, M., Hornung, U., Nanda, I., Imai, S., Sasaki, T., Shimizu, A., Asakawa, S., Hori, H., Schmid, M. & Shimizu, N. (2006). Genomic organization of the sex-determining and adjacent regions of the sex chromosomes of medaka. *Genome Research* **16,** 815–826.
Ley, S. H., Yu, M. K., Li, K. C., Tseng, C. M., Chen, C. Y., Kao, P. Y. & Huang, F. C. (1963). Limnological survey of the lakes of Yunnan Plateau. *Oceanologia et Limnologia Sinica* **5,** 87–114.
Martinez, G. M. & Bolker, J. A. (2003). Embryonic and larval staging of summer flounder (*Paralichthys dentatus*). *Journal of Morphology* **255,** 162–176.
Matsuda, M., Nagahama, Y., Shinomiya, A., Sato, T., Matsuda, C., Kobayashi, T., Morrey, C. E., Shibata, N., Asakawa, S. & Shimizu, N. (2002). DMY is a Y-specific DM-domain gene required for male development in the medaka fish. *Nature* **417,** 559–563.
McCollum, C. W., Amin, S. R., Pauerstein, P. & Lane, M. E. (2007). A zebrafish LMO4 ortholog limits the size of the forebrain and eyes through negative regulation of six3b and rx3. *Developmental Biology* **309,** 373–385.
Nanda, I., Kondo, M., Hornung, U., Asakawa, S., Winkler, C., Shimizu, A., Shan, Z., Haaf, T., Shimizu, N. & Shima, A. (2002). A duplicated copy of DMRT1 in the sex-determining region of the Y chromosome of the medaka, *Oryzias latipes*. *Proceedings of the National Academy of Sciences of the United States of America* **99,** 11778–11783.
Nornes, S., Clarkson, M., Mikkola, I., Pedersen, M., Bardsley, A., Martinez, J. P., Krauss, S. & Johansen, T. (1998). Zebrafish contains two Pax6 genes involved in eye development. *Mechanisms of Development* **77,** 185–196.
Penaz, M. (2001). A general framework of fish ontogeny: a review of the ongoing debate. *Folia Zoologica* **50,** 241–256.
Regan, C. T. (1904). On a collection of fishes made by Mr. John Graham at Yunnan Fu. *Annals and Magazine of Natural History* **7,** 190–194.
Regan, C. T. (1908). Descriptions of three new cyprinid fishes from Yunnan, collected by Mr. Graham. *Annals and Magazine of Natural History* **8,** 356–357.
Seo, H. C., Drivenes, O., Ellingsen, S. & Fjose, A. (1998). Expression of two zebrafish homologues of the murine Six3 gene demarcates the initial eye primordia. *Mechanisms of Development* **73,** 45–57.
Schulte-Merker, S. (2002). *Looking at embryos*. In *Zebrafish, A Practical Approach* (Nüsslein-Volhard, C. & Dahm, R., eds), pp. 39–58. Oxford: Oxford University Press.
Streelman, J. T., Peichel, C. L. & Parichy, D. M. (2007). Developmental genetics of adaptation in fishes: the case for novelty. *Annual Review of Ecology and Systematics* **38,** 655–681.
Westerfield, M. (2000). *The Zebrafish Book. A Guide for the Laboratory Use of Zebrafish (Danio rerio)*, 4th edn. Eugene, OR: University of Oregon Press.
Yang, L. F. (1984). The preliminary study on the original classification and distribution law of lakes on the Yunnan Plateau. *Transactions of Oceanology and Limnology* **1,** 34–39.
Yang, J. (1992). Origin and evolution of some biological characters of *Anabarilius grahami* as referred to geological development of Fuxian Lake. *Zoological Research* **13,** 353–360.
Yang, J. & Chu, X. (1987). Phylogeny of the cyprinid genus *Anabarilius*. *Zoological Research* **8,** 261–276.

